Perfluorosulfonic Acid—Tetraethoxysilane/ Polyacrylonitrile (PFSA-TEOS/PAN) Hollow Fiber Composite Membranes Prepared for Pervaporation Dehydration of Ethyl Acetate–Water Solutions

Hai-Kuan Yuan,[1] Zhen-Liang Xu,[1,2] Jiang-Huan Shi,[1] Xiao-Hua Ma[1]

[1]Membrane Science and Engineering R&D Lab, Chemical Engineering Research Center,
East China University of Science and Technology (ECUST), Shanghai 200237, People's Republic of China
[2]Key Laboratory for Ultrafine Materials of the Ministry of Education, ECUST, Shanghai 200237,
People's Republic of China

ABSTRACT: Preparation of organic-inorganic composite membranes and their pervaporation (PV) permeation and separation characteristics for the aqueous solution of ethyl acetate were described. Polyacrylonitrile (PAN) hollow fiber ultrafiltration membrane as support membrane, the mixtures of perfluorosulfonic acid (PFSA) and tetraethoxysilane (TEOS) by the sol-gel reaction as the coating solution, the PFSA-TEOS/PAN hollow fiber composite membranes by the different annealing conditions were prepared. The swelling of PFSA in ethyl acetate aqueous solutions was inhibited with addition of TEOS. The PFSA-TEOS/PAN composite membranes containing up to 30 wt % TEOS in coating solution exhibited high selectivity towards water, then the selectivity decreased and permeation flux increased with increasing the TEOS concentration more than 30 wt %. When the PFSA-TEOS/PAN composite membranes were annealed, the separation factor increased with increasing annealing temperature and time. Higher annealing temperature and longer annealing time promoted the crosslinking reaction between PFSA and TEOS in PFSA-TEOS/PAN composite membranes, leading to the enhanced selectivity towards water. For the PFSA/PAN and PFSA-TEOS/PAN composite membrane with 5 and 30 wt % TEOS annealed at 90°C for 12 h, their PV performance of aqueous solution 98 wt % ethyl acetate were as follows: the separation factors were 30.8, 254 and 496, while their permeation flux were 1430, 513 and 205 g/m^2 h at 40°C, respectively. In addition, the PV performance of PFSA-TEOS/PAN composite membranes was investigated at different feed solution temperature and concentration. © 2008 Wiley Periodicals, Inc. J Appl Polym Sci 109: 4025–4035, 2008

Key words: membranes; selectivity; separation techniques; annealing

INTRODUCTION

Pervaporation (PV) is a membrane process in which the fractionation of a liquid mixture is obtained by a partial vaporization of the mixture through a membrane into a vacuum chamber. The membrane acts as an extracting medium which works continuously without a regeneration step. Nowadays it is considered as a basic unit operation with significant potential in a wide range of applications, such as the dehydration of organic compounds, the recovery of organic compounds from water and the separation of organic mixtures, especially promising way for separation of the azeotropic,[1] or close-boiling point mixtures.[2,3] PV provides several advantages in various applications: easy process design, high selectivity, low energy consumption, and moderate cost-to-performance ratio etc.[4–10]

Ethyl acetate is a very important solvent in the chemical industry, and it is widely used in the production of perfumes, plasticizers, varnishes, synthetic resins, and adhesive agents. In general, one step in production process of ethyl acetate was to remove the water of initial product from the reactive distillation tower, and the energy-intensive distillation process was required.[11] If PV was applied to replace distillation step, it would save much energy. However, there are only few literatures reported on the PV dehydration of the ethyl acetate–water system. Salt et al.[10,12] reported data for ethyl acetate–water mixture at 30, 40, and 50°C with 97–99 wt % concentration of ethyl acetate using poly(vinyl alcohol) (PVA) crosslinked by tartaric acid (Tac). Shaban[13,14] undertook a PV study in the hydrolysis of

ethyl acetate for the initial feed composition of the ternary mixture with 10 wt % water, 40 wt % ethyl acetate, and 50 wt % acetic acid with ethanol forming as a hydrolysis product at 35, 50, 65, and 80°C, using a standard PVA membrane with a thickness of 2 μm supplied by G. F. T. of Germany. The main drawback of PVA membrane is its poor stability in aqueous solutions, and these problems have been overcome by crosslinking and modifying methods to obtain stable PVA membrane. However, the permeation flux of crosslinked PVA membrane was low, so it is necessary to develop the new membranes with high permeation flux when used to dehydrate the ethyl acetate aqueous solutions.

For polymeric PV membranes, extensive research has been performed in finding the optimized membrane. However, a major drawback of organic membranes is their limited solvent and temperature stability.[8] However, the inorganic PV membranes, mostly silica-based,[15–17] can withstand harsh chemical environments and high temperatures, which are not shown by organic membranes. The microporous silica PV membranes accompanied with mass transport of components through them were studied diffusely,[18,19] and they also seemed very effective in dehydration. The disadvantages of inorganic membranes are their brittleness and the higher production costs. Therefore, the organic–inorganic hybrid membranes, combining with the functionality of organic compounds and the stability of inorganic compounds, are expected to be the next generation, high-performance membranes in a variety of fields.[20] The hybrid membrane are made by a low-temperature, solution-based sol–gel method[21–23] and it is possible to homogeneously hybridize the organic and inorganic components to form the dense membranes. Previously, organic–inorganic hybrid membrane by the sol–gel reaction for PVA and tetraethoxysilane (TEOS),[24–26] the quaternized chitosan and TEOS,[27,28] copolymers of butyl methacrylate and vinyltriethoxysilane (P(BMA-co-VTES)) and TEOS[29,30] were prepared for dehydration of alcohol aqueous solutions, and the permeation or separation characteristics of polymer membranes was improved.

PFSA consists of a polytetrafluoroethylene (PTFE) backbone and regular spaced long perfluorovinyl ether pendant side chains terminated by a sulfonate ionic group. PFSA has excellent chemical, thermal, and mechanical properties[31] and is extensively used in chlor-alkali industry,[32] fuel cells,[33,34] and other applications.[35,36] Its chemical formula is shown as follows.

$$-(CF_2-CF_2)_{\overline{n}}(CF_2-CF)_{\overline{m}}$$
$$| $$
$$O-CF_2-CFCF_3$$
$$| $$
$$O-CF_2CF_2SO_3H$$
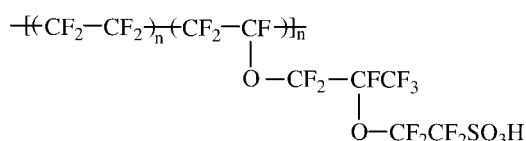
PFSA has been used for PV dehydration of isopropanol,[37] nitric acid,[38] and acetic acid[39] aqueous solutions, etc., but its selectivity towards water was very low.

To improve the separation performance of PFSA for PV dehydration of ethyl acetate aqueous solutions, the PFSA-TEOS/PAN hollow fiber composite membranes were prepared by the sol–gel reaction of mixtures of PFSA and TEOS in this study. The effects of TEOS concentration in coating solution, the annealing conditions of composite membranes, the feed solution temperature and concentration on the PV performance were investigated in detail.

EXPERIMENTAL

Materials and instrumentals

Tetraethoxysilane (TEOS) was purchased from Shanghai Ling-Feng Chemical Reagent (China). Perfluorosulfonic acid (PFSA) in granular form was self-recovered from the deteriorated ion-exchange membrane F-8020 (the product of ASAHI Glass Company, Japan) used in chlor-alkli industry, which was prepared according to the procedure by Lang et al.[40] All other solvents and reagents were obtained from Shanghai Chemical Reagent Company (China).

Polyacrylonitrile (PAN) hollow fiber ultrafiltration support membranes (self-made, pure water flux: 14 L/(m² h Bar)).

Gas chromatograph (GC Chromatography GC7890 T, China) equipped with a thermal conductivity detector (TCD) and a GDX-102 packed column, FT-IR spectrometer (Nicolet 6700, America), scanning electron microscope (SEM) (JEOL, JSM-6360 LV, Japan), and a contact angle meter (JC2001, China) were used.

Preparation of PFSA-TEOS/PAN hollow fiber composite membrane

PFSA in granular form was dissolved in an aqueous solution of 80 wt % ethylene glycol (EG) at 60°C to make 5 wt % coating solution, then the insoluble impurities were removed using a glass filter. After the prescribed amount of TEOS per a weight of mixtures of PFSA and TEOS was mixed with the PFSA in EG aqueous solution at 25°C, 1M HCl was added to the mixtures of PFSA and TEOS as an acid catalyst for the sol–gel reaction, which was the preparation of coating solution. PAN hollow fiber membranes were immersed in the coating solution for 30 s by dip-coating method and then dried at room temperature. Every fiber was coated twice, after the membranes were coated for the second time, the membranes were hanged inversely when being dried. The final PFSA-TEOS/PAN hollow fiber com-

posite membranes were obtained after being annealed at different temperature and time in a vacuum drying oven.

PV process for dehydration of ethyl acetate–water solutions

Figure 1 illustrates the schematic diagram of the PV apparatus. The hollow fiber membrane cell has three modules, and each module consists of three to five fibers with lengths of 20 cm. The permeate side was maintained at a vacuum pressure (2.6 kPa) using a vacuum pump. The permeate vapor sample was collected after being condensed in the cold traps using liquid nitrogen.

Permeation flux (J, g/m^2 h) of hollow fiber membranes is defined as follows:

$$ J = \frac{W}{t \times A} \tag{1} $$

where W is the total amount of permeate (g), t the experimental time interval (h), and A the total outer surface area of hollow fiber membranes (m^2). The composition of permeate and feed solution were analyzed using a gas chromatograph at a temperature of 120°C.
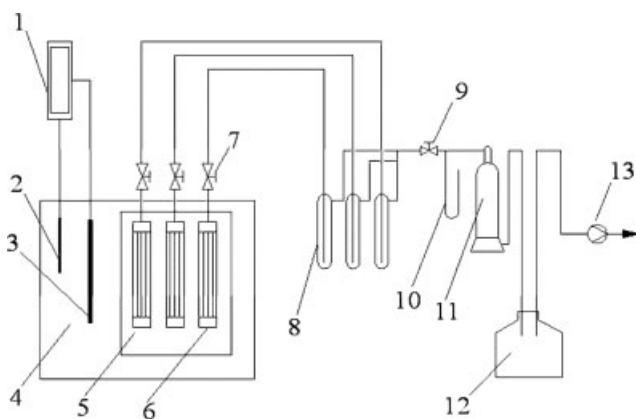
The separation factor (α) is defined by:

$$ \alpha = \frac{(Y_W/Y_{EA})_{\text{permeate}}}{(X_W/X_{EA})_{\text{retentate}}} \tag{2} $$

where Y_W, Y_{EA}, X_W, and X_{EA} are the weight fractions of water and ethyl acetate in the permeate and retentate, respectively.

Contact angle measurements

To measure the contact angles of PFSA/PAN and PFSA-TEOS/PAN hollow fiber composite mem-

Figure 1 Schematic diagram of the PV process apparatus. 1. temperature controller; 2. thermocouple; 3. heater; 4. water bath; 5. feed solution tank; 6. membrane module; 7. vacuum valve; 8. cold trap; 9. stopcock; 10 manometer; 11. absorbed column; 12. buffer; 13. vacuum pump.
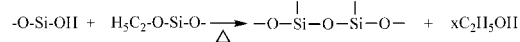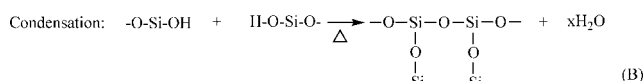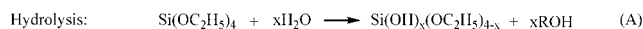
Scheme 1 Hydrolysis and condensation reaction for TEOS.

branes, the PFSA/PAN and PFSA-TEOS/PAN flat composite membranes were prepared. The contact angles for methylene iodide on the surface of PFSA and PFSA-TEOS composite membranes were measured using a contact angle meter (JC2001, China) at room temperature. The contact angles, θ, were determined by eq. (3).

$$ \theta = \cos^{-1}\{(\cos\theta_a - \cos\theta_r)/2\} \tag{3} $$

where θ_a and θ_r are the advancing contact angle and the receding contact angle, respectively.

Morphology of PFSA-TEOS/PAN composite membranes

SEM was used to visualize the outer surface and cross section morphology photographs of PAN support fibers and PFSA-TEOS/PAN composite membranes. The cross section of hollow fibers for the SEM was prepared after breaking the membranes in liquid nitrogen to avoid destroying the structure of fibers. All samples were sputter-coated with gold before analysis.

RESULTS AND DISCUSSION

Formation of PFSA-TEOS top layer of PFSA-TEOS/PAN composite membrane

Scheme 1 shows the process of the polycondensation reaction of TEOS.[27,41] In the first step of process of preparing the PFSA-TEOS/PAN composite membrane, TEOS was hydrolyzed in the presence of an acid catalyst (A), which led to the formation of silanol groups. The resulting silanol groups converted to siloxane bonds due to the dehydration or dealcoholysis reaction (B) with other silanol groups or ethoxy groups. These reactions led to the formation of cohesive siloxane domains in the top layer of PFSA-TEOS/PAN composite membranes. Because these siloxane domains were dispersed in the top layer, the silanol groups in the siloxane domains and the hydroxyl groups in PFSA formed hydrogen and covalent bonds, which were the crosslinked points, as illustrated in Scheme 2.
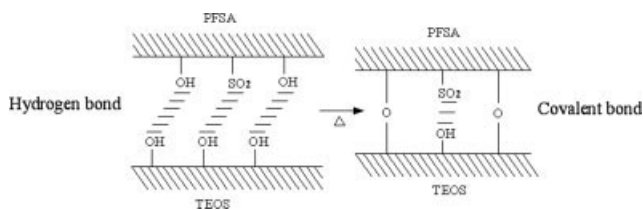
Scheme 2 Tentative illustration for the interaction between PFSA and TEOS.

## FT-IR analysis of top layer of PFSA-TEOS/PAN composite membrane

Figure 2 shows the FT-IR spectra of recovered PFSA sample and top layer of PFSA-TEOS/PAN composite membrane with 30 wt % TEOS. PFSA has strong bands at 1155 and 1230 cm^{-1} which correspond to the C-F stretching modes. The peaks at 1059 and 1084 cm^{-1} correspond to the Si—O—Si stretching vibration, and the broad band near 3421 cm^{-1} corresponds to the structural hydroxyl groups, and little physisorbed water. These results suggest the formation of a crosslinked structure due to the sol–gel reaction, in which the silanol groups in the tetrasilanol silane (TSS) produced by the hydrolysis of TEOS reacted with the hydroxyl groups in the PFSA molecule.

Effect of the TEOS concentration on PV performance of PFSA-TEOS/PAN composite membranes

Figure 3 shows the effect of the TEOS concentration in coating solution on the separation factor (α) and the permeation flux (J) of an aqueous solution of 98 wt % ethyl acetate through the PFSA/PAN and PFSA-TEOS/PAN composite membranes by PV at
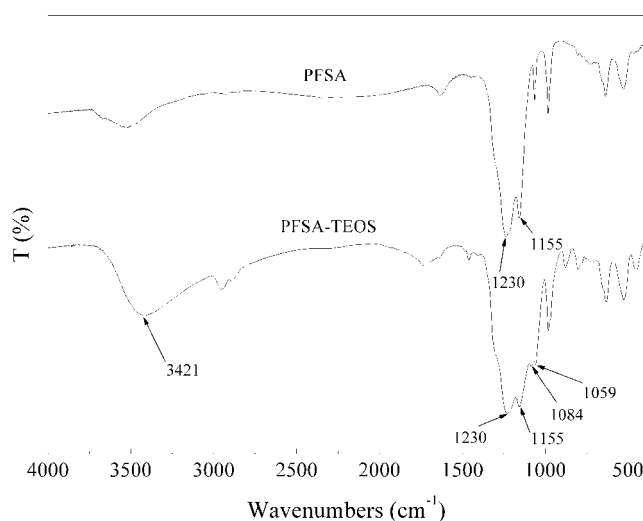

Figure 2 FT IR spectra of recovered PFSA and top layer of the PFSA-TEOS/PAN composite membrane.
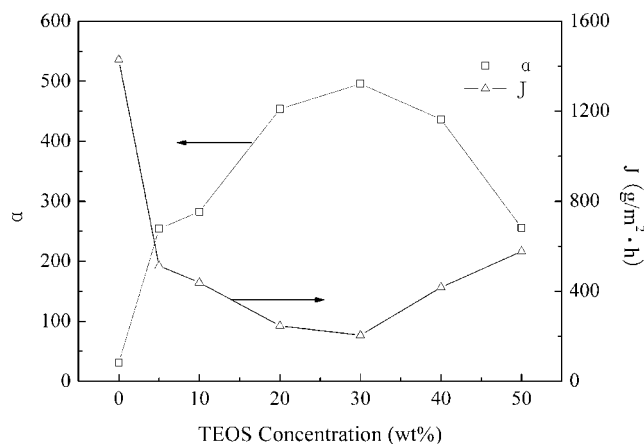
Figure 3 Effect of the TEOS concentration on the PV performance for the aqueous solution of 98 wt % ethyl acetate through the PFSA-TEOS/PAN composite membranes at 40°C. The annealing temperature was 90°C, annealing time 12 h.

40°C. The annealing temperature was 90°C, and annealing time 12 h. As shown in Figure 3, PFSA/PAN composite membrane had high permeation flux, and low separation factor, while for PFSA-TEOS/PAN composite membrane, the separation factor increased remarkably with TEOS concentration up to 30 wt % in coating solution, however, its selectivity towards water decreased when the TEOS concentration was further increased. Increase in the separation factor may be because the top layer became denser and the degree of swelling of PFSA was decreased remarkably with increasing TEOS concentration. However, decrease in the separation factor of PFSA-TEOS/PAN composite membrane containing more than 30 wt % TEOS may be attributed to the cohesive effect of TEOS. The organic and inorganic components were homogeneously mixed in the composite membranes at low TEOS concentration, whereas cohesive bodies of TEOS are formed and a microphase-separated structure was obtained for membranes at high TEOS concentration, where the crosslinking reaction between PFSA and TEOS was less favored because of precedence of the polycondensation reaction among the TEOS molecules. Therefore, an increase in the permeation flux and a decrease in the water–ethyl acetate selectivity were observed. The addition of TEOS to PFSA for preparation of composite membrane was suitable and effective for the separation of the ethyl acetate–water solution, when the TEOS concentration in coating solution was below 30 wt %.

Figure 4 shows effect of TEOS concentration in coating solution on the contact angles for methylene iodide on the surface of PFSA/PAN and PFSA-TEOS/PAN composite membranes. Since methylene iodide was used for the measurement of the contact
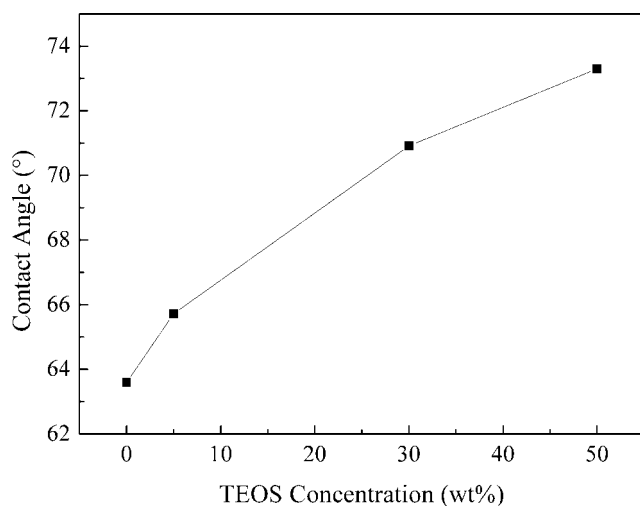
Figure 4 Effect TEOS concentration on contact angle for methylene iodide on the surface of PFSA/PAN and PFSA-TEOS/PAN composite membranes.

angle of the membrane surface, a higher contact angle implies a more hydrophilic membrane surface. As seen in Figure 4, with increasing TEOS concentration, the contact angle increased. This result suggests that the surface of the membrane became more hydrophilic, which is helpful to increase the selectivity of PFSA-TEOS/PAN composite membranes, and also supports the results in Figure 3 when TEOS concentration of PFSA-TEOS/PAN composite membrane was less than 30 wt %.

The membrane morphology of outer surfaces of PFSA-TEOS/PAN composite membranes with different TEOS concentration in coating solutions was shown in Figure 5. The TEOS concentration in PFSA-TEOS coating solution has obvious effect on the surfaces of composite membranes. The outer surface of PFSA/PAN composite membrane is rough as shown in Figure 5(B), and the addition of TEOS makes the outer surfaces of composite membranes smooth and
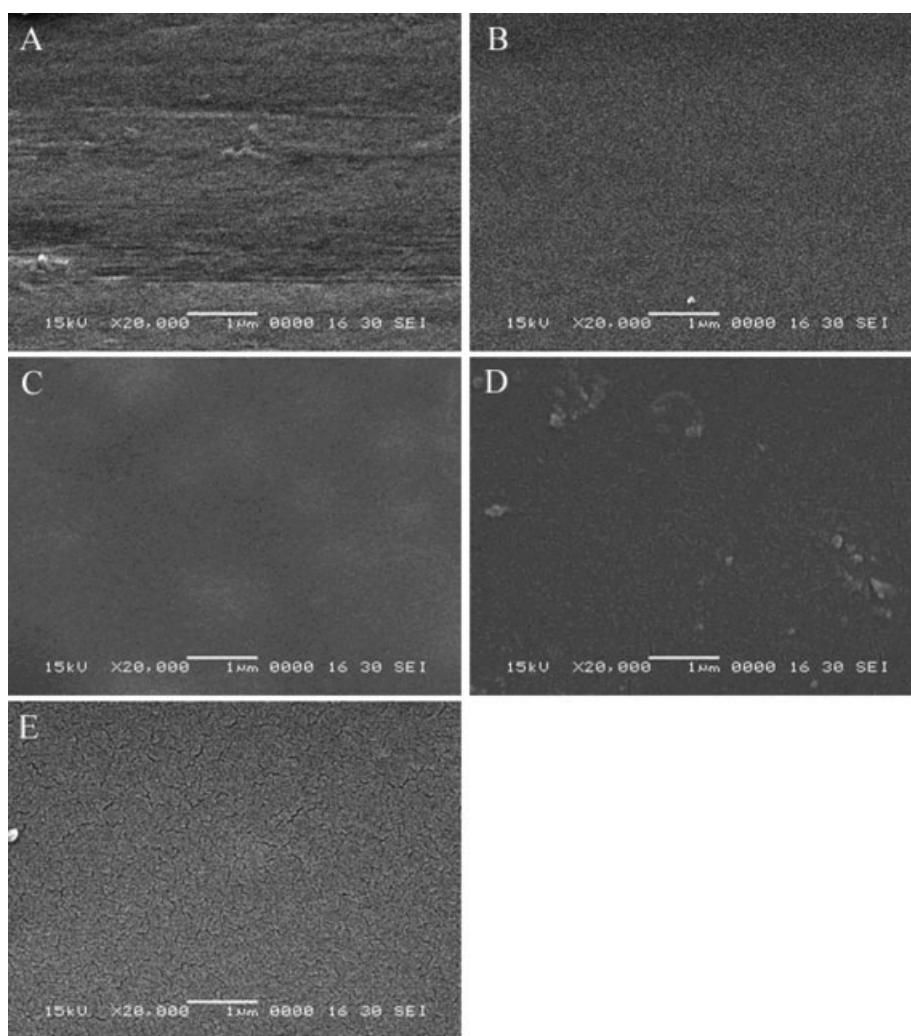
Figure 5 SEM photographs of Outer surface of PFSA-TEOS/PAN composite membranes with different TEOS concentration in coating solution. A: PAN support membrane; B: PFSA/PAN; C: PFSA-TEOS/PAN (5 wt % TEOS); D: PFSATEOS/PAN (30 wt % TEOS); E: PFSA-TEOS/PAN (50 wt % TEOS).
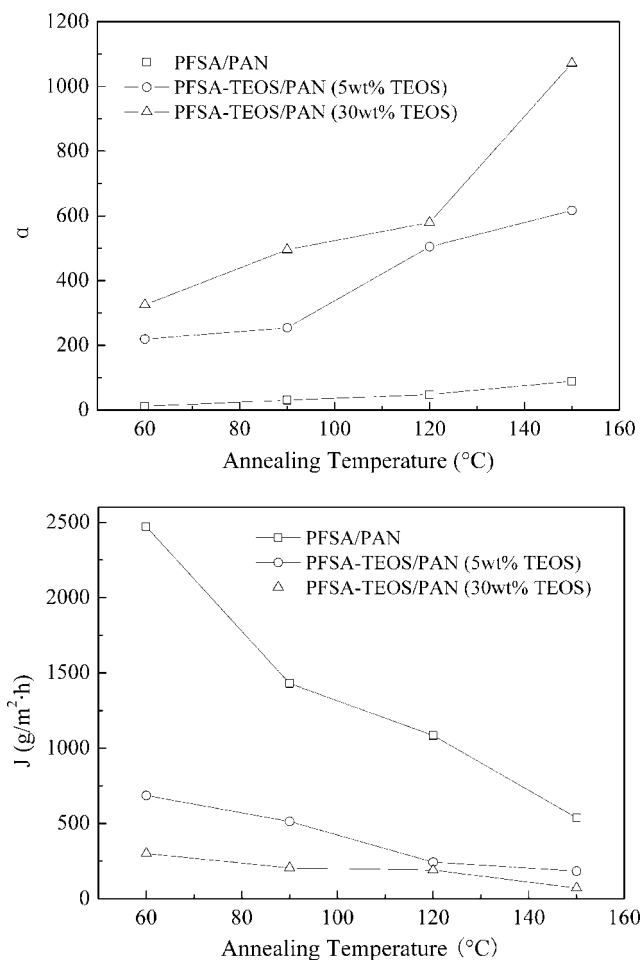
Figure 6 Effect of the annealing temperature on PV performance for the aqueous solution of 98 wt % ethyl acetate through the PFSA/PAN and PFSA-TEOS/PAN composite membranes with 5 and 30 wt % TEOS at 40°C. The annealing time was 12 h.

dense gradually. However, many cracks appear on the outer surface of PFSA-TEOS/PAN composite membrane with 50 wt % TEOS. An increase of the TEOS concentration in coating solution enhances the degree of compactness of top layer and weakens pliability of PFSA at the same time, which results in the appearance of some cracks when TEOS concentration is too high. These cracks also may be the reason for the decrease of the separation factor and the increase of permeation flux.

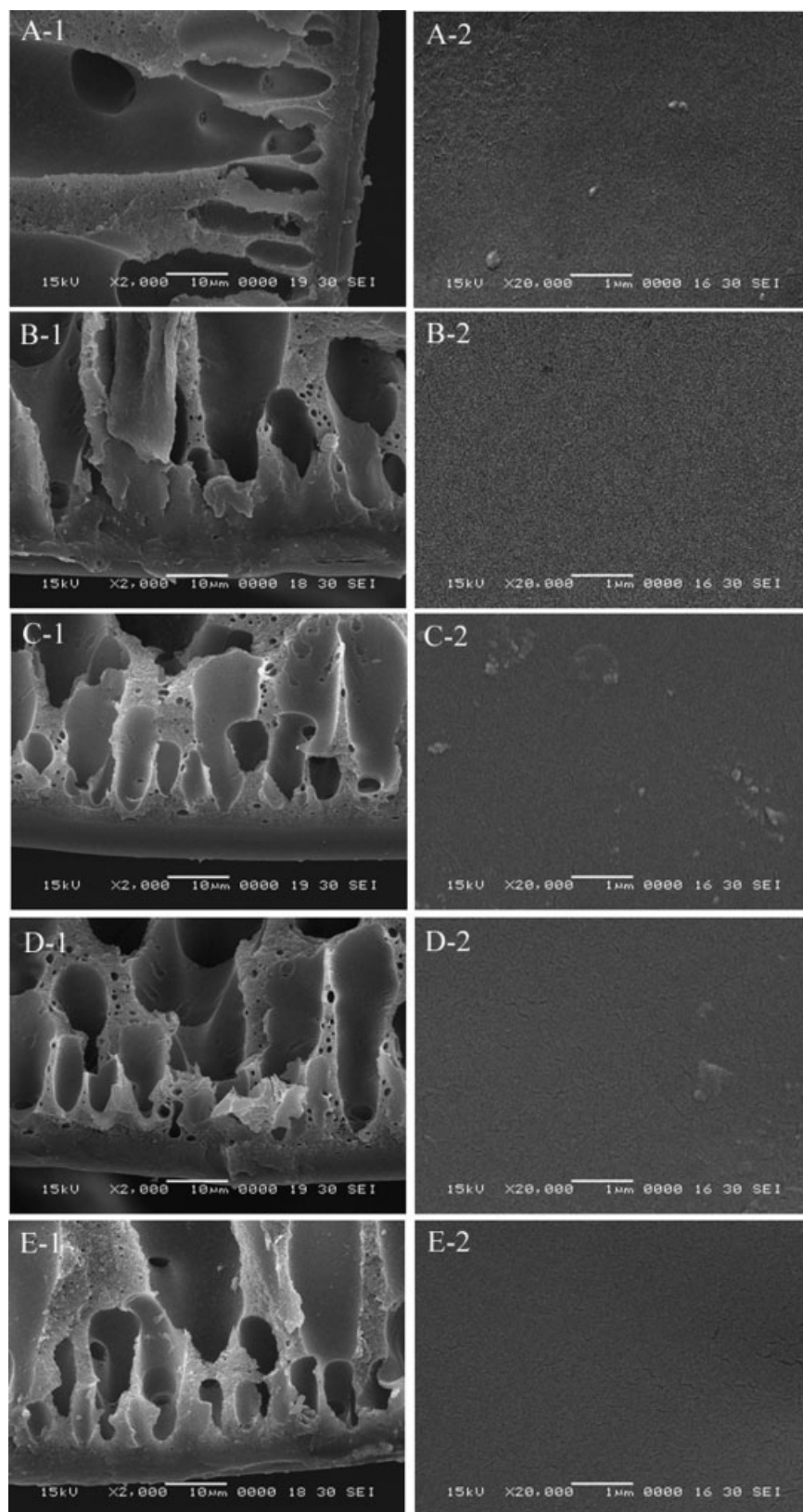### Effect of annealing on PV performance of PFSA/PAN and PFSA-TEOS/PAN composite membranes

It has been reported that the polycondensation reaction of TEOS strongly depends on the annealing temperature and time,[25,42] and the structure of the resulting membranes was significantly influenced by these factors. Therefore, to prepare composite mem-

branes with better permeation and separation characteristics, the effects of annealing on PV performance were investigated.
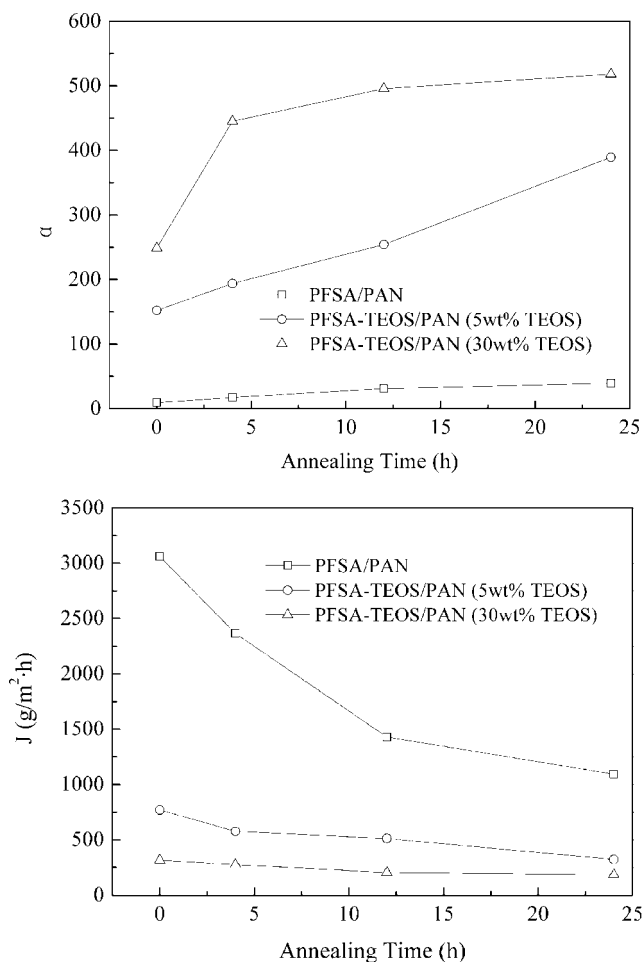
Figure 6 shows effect of the annealing temperature on the separation factor (α) and the permeation flux (J) for the aqueous solution of 98 wt % ethyl acetate through the PFSA/PAN and PFSA-TEOS/PAN composite membranes with 5 and 30 wt % TEOS. In this case, the annealing time was fixed for 12 h and the annealing temperatures were 60, 90, 120, and 150°C, respectively. As shown in Figure 6, the PFSA-TEOS/PAN composite membrane had better separation characteristics than the PFSA/PAN composite membrane over the entire range of annealing temperatures. The separation factor and the permeation flux for PFSA/PAN and PFSA-TEOS/PAN composite membranes were the functions of annealing temperature, as the annealing temperature increased, the separation factor increased while the permeation flux decreased. When the annealing temperature was high, the crosslinking reaction between PFSA and TEOS molecules and the polycondensation reaction of TEOS in PFSA-TEOS/PAN composite membranes proceeded completely, which resulted in smaller network pore and aggregate pore size and decreased fractional free volume. Those effects made the separation factor higher and permeation flux smaller. However, the apparent fractional free volume increased with increasing annealing temperature, which was helpful to increase permeation flux of composite membranes. The coupling effects made the decreasing extent of permeation flux smaller.[43,44] So the separation factor of the PFSA-TEOS/PAN composite membranes increased remarkably with increasing the annealing temperature, while the decrease of permeation flux of PFSA-TEOS/PAN composite membrane was smaller.

As seen in Figure 7, the coating layers with the thickness of about 2–5 μm were clearly found on the pictures for near outer surfaces. With increasing annealing temperature, the traces of juncture in cross sections between coating layer and the support disappear gradually, and the outer surface of PFSA-TEOS/PAN composite membrane become smoother, which indicates the composite membranes become denser with increasing annealing temperature. The denser top layer of PFSA-TEOS/PAN composite membrane makes an increase of separation factor, which is in agreement with the experimental results.

Figure 8 shows the effect of the annealing time on the separation factor (α) and permeation flux (J) of PFSA/PAN and PFSA-TEOS/PAN composite membranes with 5 and 30 wt % TEOS. In Figure 8 the annealing temperature of PFSA/PAN and PFSA-TEOS/PAN composite membranes was fixed at 90°C, and the annealing time was changed. The effect of annealing time on PV properties of PFSA-

Figure 7 SEM photographs of PFSA-TEOS/PAN composite membrane with 30 wt % TEOS at different annealing temperature. A: unannealed; B: 60°C; C: 90°C; D: 120°C; E: 150°C.

Figure 8 Effect of annealing time on PV performance for the aqueous solution of 98 wt % ethyl acetate through the PFSA/PAN and PFSA-TEOS/PAN composite membranes with 5 and 30 wt % TEOS at 40°C. The annealing temperature was 90°C.

TEOS/PAN composite membranes followed the same trends as annealing temperature. As seen in Figure 8, the separation factor of all membranes increased, while their permeation flux decreased with increasing annealing time. From these results, it is concluded that the crosslinking reaction between the PFSA and TEOS and the polycondensation reaction of TEOS proceeded more completely with increasing annealing time, resulting in smaller network pore and aggregate pore size and decreased fractional free volume.

For all the composite membranes, the annealed PFSA/PAN and PFSA-TEOS/PAN composite membranes had higher separation factor for water perm-selectivity than those of untreated composite membranes. As shown in Figures 6 and 8, for the PFSA-TEOS/PAN composite membrane with 30 wt % TEOS, the separation factor (α) was changed from 325 to 1070 with increasing annealing temperature

from 60 to 150°C, while that was changed from 249 to 518 with increasing annealing time from 0 to 24 h. This fact suggests that varying the annealing temperature was more effective for improving separation characteristics of the PFSA-TEOS/PAN composite membrane than varying the annealing time.

Effect of the feed solution temperature on PV performance of PFSA/PAN and PFSA-TEOS/PAN composite membranes

The effect of the feed solution temperature on the PV performance of the PFSA/PAN and PFSA-TEOS/PAN composite membranes for aqueous solution of 98 wt % ethyl acetate is shown in Figure 9, the annealing temperature of composite membranes was 90°C, the annealing time 12 h. In general, the permeation flux increases and the separation factor decreases, as the feed solution temperature increases.
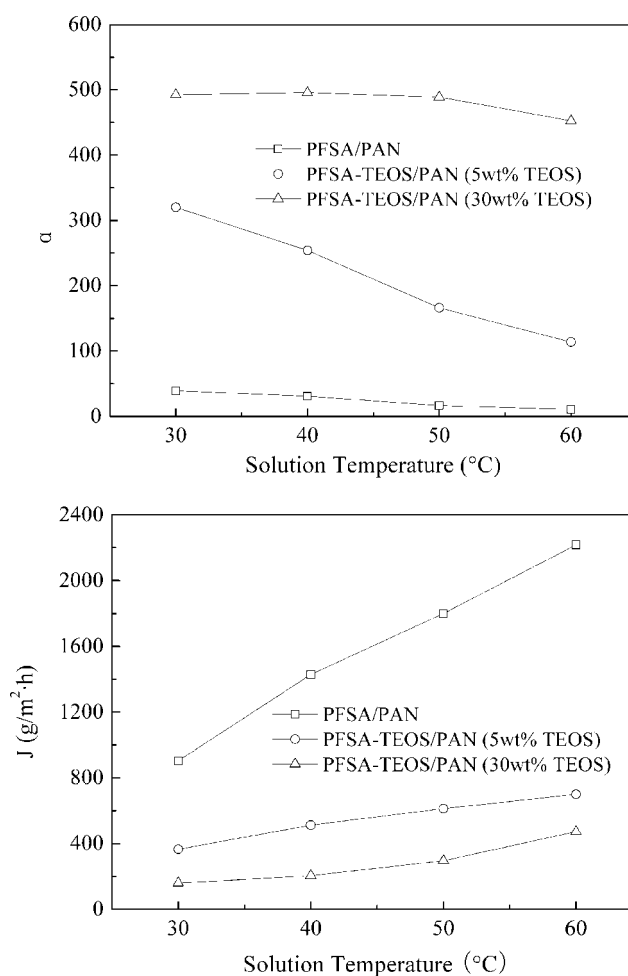
Figure 9 Effect of the feed solution temperature on PV performance for the aqueous solution of 98 wt % ethyl acetate through the PFSA/PAN and PFSA-TEOS/PAN composite membranes with 5 and 30 wt % TEOS. The annealing temperature was 90°C, annealing time 12 h.
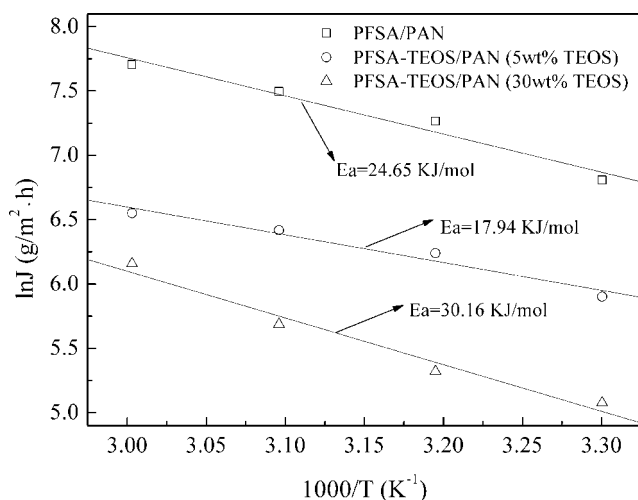
Figure 10 The activation energy required for pervaporation permeation of 98 wt % ethyl acetate aqueous solution through PFSA/PAN and PFSA-TEOS/PAN composite membranes.

The permeation and separation behavior of PFSA/PAN and PFSA-TEOS/PAN composite membranes matched well with the general behavior with increasing feed solution temperature from 30 to 60°C. As feed solution temperature increased, the mobility of top layer of PFSA-TEOS/PAN composite membranes was enhanced, and the free volume within the polymer matrix was expanded. The generated extra free volume was helpful to increase the sorption and diffusion rates of permeate molecules. Thus, the permeation flux increased. This type of increase in free volume of the polymer matrix will also result in an easy transport of organic component. Consequently, the membrane selectivity to water will be reduced.

The activation energy (ΔE_a) lumps together the effects of sorption, diffusion, and saturation pressure on the driving force. For instance, diffusion as an activated process increases with temperature due to higher mobility of the molecules. The activation energy required for permeation of 98 wt % ethyl acetate aqueous solution through PFSA/PAN and PFSA-TEOS/PAN composite membranes was calculated on the basis of the Arrhenius equation, as shown in Figure 10.

The activation energy (ΔE_a) of PFSA/PAN, PFSA-TEOS/PAN composite membranes with 5 and 30 wt % TEOS were 24.65, 17.94, and 30.16 KJ/mol, respectively. The activation energy indicated that temperature variation affected the permeation behavior of components in membranes significantly, and the presence of TEOS in PFSA-TEOS coating solution formed a dense top layer of PFSA-TEOS/PAN composite membranes.

Effect of the feed concentration on PV performance of PFSA/PAN and PFSA-TEOS/PAN composite membranes

Figure 11 shows the effect of changes in the feed concentration on the PV performance of ethyl acetate–water mixture at 40°C. The composite membranes were annealed at 90°C for 12 h. The feed concentration ranged from 97 to 99 wt % of ethyl acetate aqueous solution in feed solution, which was chosen by considering the azeotropic mixture of ethyl acetate and water with miscible phase occurring at compositions more than 97 wt % ethyl acetate. It was found that the permeation flux of composite membranes decreased whereas the separation factor increased gradually as the ethyl acetate in feed solution increased. The reason is that the swelling degree of PFSA, the mobility of PFSA chains, and the free volume of PFSA-TEOS top layer decreased with increasing ethyl acetate concentration in the feed, which led the sorption and diffusion of water and ethyl acetate to decline. As reported by Bartels and
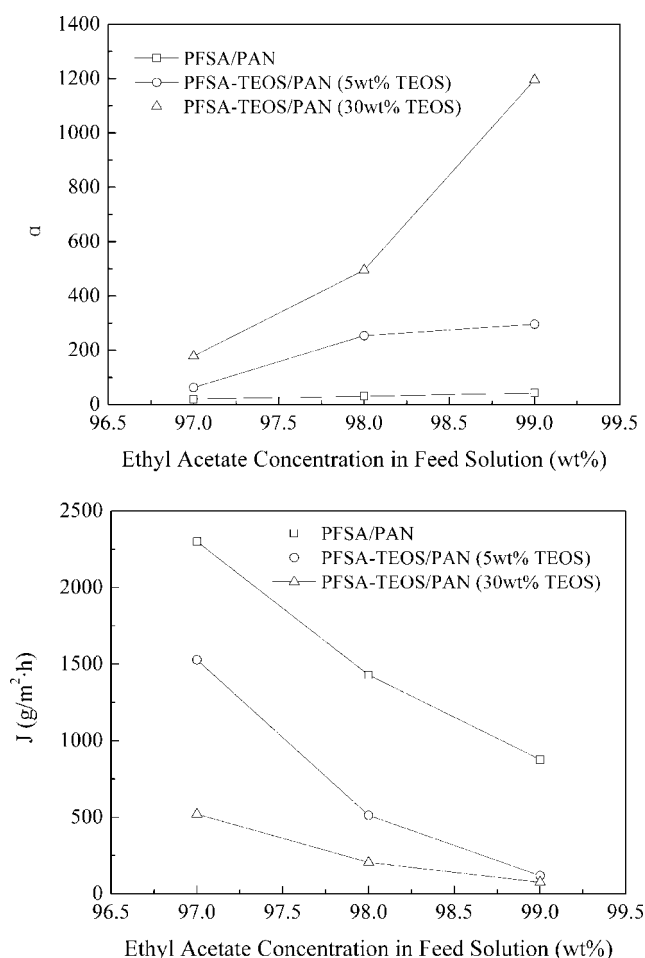
Figure 11 Effect of the solution concentration on PV performance through the PFSA/PAN and PFSA-TEOS/PAN composite membranes with 5 and 30 wt % TEOS at 40°C. The annealing temperature was 90°C, annealing time 12 h.

TABLE I
Permeation and Separation Characteristics for Pervaporation Dehydration of Ethyl Acetate Aqueous Solutions Through Some Polymer Membranes[a]

Membrane	Feed comp. (wt%)	T (°C)	J (g/m² h)	$\alpha_{H_2O/EAc}$	Ref.
PVA (cross-linked by Tac)	EAc/H$_2$O = 98/2	30	31.99 (J_W)	5202	10,12
Standard PVA (G.F.T.)	EAc/HAc/H$_2$O = 40/50/10	65	46.7 (J_W)	72	13,14
PFSA/PAN[b]	EAc/H$_2$O = 98/2	40	1430	30.8	This study
PFSA-TEOS/PAN (5 wt % TEOS)[b]	EAc/H$_2$O = 98/2	40	513	254	This study
PFSA-TEOS/PAN (30 wt % TEOS)[b]	EAc/H$_2$O = 98/2	40	205	496	This study

[a] EAc-Ethyl acetate; HAc-acetic acid; J_W-the water flux.
[b] Annealed at 90°C, 12 h.

Li,[45,46] the characteristics of the sorption depended on the difference between the affinity of the components towards the polymer, the mutual interactions with the components, and the way the interactions with the polymer of each component affected the interactions of the other penetrates with the polymer. In addition, ethyl acetate molecules with larger size would experience much bigger diffusion resistance. Therefore, the separation factor increased accompanying with the decrease in permeation flux with increasing the ethyl acetate concentration in feed solution. For instance, the separation factor (α) of PFSA-TEOS/PAN composite membrane with 30 wt % TEOS was changed from 179 to 1196, while its permeation flux (J) was decreased from 520 to 75 g/m² h with increasing the feed concentration of ethyl acetate from 97 to 99 wt %.

Performance of PFSA-TEOS/PAN composite membranes

In Table I, the permeation and separation characteristics for an ethyl acetate aqueous solution through water permselective polymer membranes during PV are summarized. The permeation fluxes for PFSA/PAN and PFSA-TEOS/PAN composite membranes are relatively higher than those for other membranes, although the separation factor of PFSA/PAN and PFSA-TEOS/PAN composite membranes are smaller. Compared with PFSA/PAN composite membrane, the separation factor of the PFSA-TEOS/PAN composite membrane was significantly enhanced. These results suggest that the addition of TEOS to PFSA is very effective, and it controlled the swelling of PFSA in aqueous solution and enhanced the separation factor consequently. This study suggests a possibility of appearance of novel PFSA-TEOS/PAN composite membranes.

CONCLUSIONS

The PFSA-TEOS/PAN composite membranes were prepared by the sol–gel reaction of PFSA and TEOS for dehydration of ethyl acetate aqueous solutions. The swelling of PFSA in ethyl acetate aqueous solu-

tions was inhibited with addition of TEOS. The PFSA-TEOS/PAN composite membranes containing up to 30 wt % TEOS in coating solution exhibited higher selectivity towards water, however, its selectivity decreased when the TEOS concentration was further increased, and the permeation flux increased again. With increasing annealing temperature and time of composite membranes, the separation factor increased, while the permeation flux decreased. For the PFSA/PAN and PFSA-TEOS/PAN composite membrane with 5 and 30 wt % TEOS annealed at 90°C for 12 h, their PV performance of aqueous solution 98 wt % ethyl acetate were as follows: the separation factors were 30.8, 254, and 496, while their permeation flux were 1430, 513, and 205 g/m² h at 40°C, respectively. In addition, the feed solution temperature and concentration had remarkable effects on the PV performance of PFSA/PAN and PFSA-TEOS/PAN composite membranes. From the above results, it is clear that the novel PFSA-TEOS/PAN composite membrane could offer potential for dehydration of ethyl acetate–water binary solutions.

References

1. Psaume, R.; Aurell, Y.; Mora, J. C.; Bersillon, J. L. J Membr Sci 1988, 36, 373.
2. Blume, I.; Wijmans, J. G.; Baker, R. W. J Membr Sci 1990, 49, 253.
3. Fang, Y.; Pham, V. A.; Matsuura, T.; Santerre, J. P.; Narbaitz, R. M. J Appl Polym Sci 1994, 54, 1937.
4. Nijhius, H. H.; Mulder, M. H. V.; Smolders, C. A. J Appl Polym Sci 1993, 4, 2227.
5. Koops, G. H.; Smolders, C. A. Pervaporation Membrane Separation Processes; Wilky: New York, 1991; p 253.
6. Rhim, J. W.; Sohn, M.; Lee, K. H. J Appl Polym Sci 1994, 52, 1217.
7. Smitha, B.; Suhanya, D.; Sridhar, S.; Ramakrishna, M. J Membr Sci 2004, 241, 1.
8. Feng, X.; Huang, R. Y. M. Ind Eng Chem Res 1997, 36, 1048.
9. Zhang, S.; Drioli E. Sep Sci Technol 1995, 30, 1.
10. Salt, Y.; Hasanöglu, A.; Dinçer, S. Chem Eng Commun 2003, 190, 564.
11. Lee, H. Y.; Huang, H. P.; Chien, I. L. J Process Control 2007, 17, 363.
12. Salt, Y.; Hasanöglu, A.; Salt, İ.; Keleser, S.; Özkan, S.; Dinçer, S. Vacuum 2005, 79, 215.
13. Shaban, H. I. Eur Polym Mater 1998, 34, 955.

14. Shaban, H. I. J Appl Polym Sci 1998, 70, 2361.

15. Verkerk, A. W.; Male, P. V.; Vorstman, M. A. G.; Keurentjes, J. T. F. J Membr Sci 2001, 193, 227.

16. Verkerk, A. W.; Male, P. V.; Vorstman, M. A. G.; Keurentjes, J. T. F. Sep Purif Technol 2001, 22/23, 689.

17. Veen, H. M. V.; Delft, Y. C. V.; Engelen, C. W. R.; Pex, P. P. A. C. Sep Purif Technol 2001, 22/23, 361.

18. Broeke, L. J. P.; Kapteijn, F.; Moulijn, J. A. Chem Eng Sci 1999, 54, 259.

19. Bettens, B.; Dekeyzer, S.; Bruggen, B. V. D.; Degrève, J.; Vandecasteele, C. J Phys Chem B 2005, 109, 5216.

20. Chujo, Y.; Saegusa, T. Adv Polym Sci 1992, 100, 11.

21. Juangvanich, N.; Mauritz, K. A. J Appl Polym Sci 1998, 67, 1799.

22. Mauritz, K. A.; Payne, J. T. J Membr Sci 2000, 168, 39.

23. Cornelius, C.; Hibshman, C.; Marand, E. J Membr Sci 2003, 211, 25.

24. Uragami, T.; Okazaki, K.; Matsugi, H.; Miyata, T. Macromolecules 2002, 35, 9156.

25. Uragami, T.; Mastugi, H.; Miyata, T. Macromolecules 2005, 38, 8440.

26. Guo, R. L.; Hu, C. L.; Pan, F. S.; Wu, H.; Jiang, Z. Y. J Membr Sci 2006, 281, 454.

27. Uragami, T.; Katayama, T.; Miyata, T.; Tamura, H.; Shiraiwa, T.; Higuchi, A. Biomacromolecules 2004, 5, 1567.

28. Liu, Y. L.; Hsu, C. Y.; Su, Y. H.; Lai, J. Y. Biomacromolecules 2005, 6, 368.

29. Ohshima, T.; Matsumoto, M.; Miyata, T.; Uragami, T. Macromol Chem Phys 2005, 206, 473.

30. Ohshima, T.; Matsumoto, M.; Miyata T.; Uragami T. Macromol Chem Phys 2005, 206, 1683.

31. Carla, H. W. J Membr Sci 1996, 120, 1.

32. Yeo, R. S.; Mcbreen, J.; Kissel, G.; Kulesa, F.; Srinivasan, S. J Appl Electrochem 1980, 10, 741.

33. Ma, Z. Q.; Cheng, P.; Zhao, T. S. J Membr Sci 2003, 215, 327.

34. Shao, Z. G.; Wang, X.; Hsing, I. M. J Membr Sci 2002, 210, 147.

35. Jiang, J. S.; Greenberg, D. B.; Fried, J. R. J Membr Sci 1997, 132, 255.

36. Krishnan, M.; White, J. R.; Fox, J. R.; Bard, A. J. J Am Chem Soc 1983, 105, 7002.

37. Cabasso, I.; Liu, Z. Z.; Makenzie, T. J Membr Sci 1986, 28, 109.

38. Scott, S. K.; Douglas, W. J.; Chen, W. J. J Membr Sci 2002, 203, 155.

39. Ray, S. K.; Sawant, S. B.; Joshi, J. B. J Membr Sci 1998, 138, 1.

40. Lang, W. Z.; Xu, Z. L.; Yang, H.; Tong, W. J Membr Sci 2007, 288, 123.

41. Sakka, S.; Ito, S.; Kamiya, K. J Non-Cryst Solids 1985, 71, 311.

42. Einarsrud, M. A.; Kirkedelen, M. B.; Nilsen, E.; Mortensen, K.; Samseth, J. J Non-Cryst Solids 1998, 231, 10.

43. Peng, F. B.; Lu, L. Y.; Sun, H. L.; Jiang, Z. Y. J Membr Sci 2006, 281, 600.

44. Peng, F. B.; Lu, L. Y.; Hu, C. L.; Wu, H.; Jiang, Z. Y. J Membr Sci 2005, 259, 65.

45. Bartels, C. C.; Tusel, E. L.; Lichterthaler, R. N. J Membr Sci 1992, 70, 75.

46. Li, B. B.; Xu, Z. L.; Qusay, F. A.; Li, R. Desalination 2006, 193, 171.